Available online at www.sciencedirect.com
ScienceDirect
Catalysis Today 129 (2007) 380–390
CATALYSIS TODAY
www.elsevier.com/locate/cattod

A dual functional staged hydrogen purifier for an integrated fuel processor–fuel cell power system

David C. Calabro [a,*], Randall D. Partridge [a], Paul J. Berlowitz [a], Barbara Carstensen [a], Harold W. Deckman [a], Philip L. DaPrato [b], Frank Hershkowitz [a], Richard F. Socha [a]

[a] *ExxonMobil Research and Engineering Company, Corporate Strategic Laboratory, 1545 Route 22 East, Annandale, NJ 08801, USA*
[b] *Ambitech Engineering Corporation, 22 Church Street, P.O. Box 88, Liberty Corner, NJ 07938, USA*

Abstract

This paper describes the operation of a dual functional, membrane/catalytic CO_x methanator, hydrogen purifier that is well-suited for an integrated fuel processor/fuel cell power system. In combination with a pressure swing reformer (PSR) and a PEMFC, the system provides high overall efficiency and portability for distributed power or onboard vehicle use. Gas testing results illustrate the ability of the purifier to produce fuel cell purity hydrogen at peak power flux. The durability of this purifier is shown by its ability to meet target hydrogen purity even with a membrane that permeates >3000 ppm CO. Gas purge streams from both fuel cell electrodes are combined with the membrane retentate and combusted in the PSR combustion cycle to provide heat for the reforming reaction leading to high thermal efficiency. Most significantly, it is shown that staging of this purifier, enables recovery of some fraction of the purified hydrogen at pressures substantially approaching that of the feed hydrogen partial pressure. This creates an onboard source of high pressure hydrogen to be optionally fed to a storage device for use during vehicle startup, or to the fuel cell, either directly or via the storage device, under high power load conditions. The beneficial impact of this two-stage, dual functional purifier on membrane cost, dependability and fuel processor/fuel cell integration, will be discussed.

Keywords: Staged hydrogen recovery; Onboard storage; Membrane/methanotor; Pressure swing reforming

1. Introduction

The production of electricity from hydrogen requires three major process steps. First, since molecular hydrogen does not exist naturally in any substantial amount it must be generated. This is most economically done via the steam reforming or partial oxidation of hydrocarbon sources. Since this produces a ''synthesis gas'' mixture, the hydrogen must undergo substantial purification prior to use. Finally, high purity hydrogen is reacted with oxygen in a fuel cell to generate electricity and water. These three steps constitute the heart of a hydrogen-based energy technology.

Multiple technologies exist for all three of these steps. Diverse scenarios have also been identified for integrating these steps into a power system. A key parameter in designing these systems is the decision to either co-locate or physically separate the three key process steps. Co-location of the process steps may be more desirable for relatively small, portable, distributed power systems if a local, low cost source of purified hydrogen is not otherwise available. Examples of this scenario include an integrated reformer, hydrogen purifier and fuel cell running off either grid natural gas to generate residential power, or gasoline/diesel for vehicle power [1,2]. This paper discusses an integrated fuel processor–fuel cell system for distributed power generation. The focus of the paper is primarily on the hydrogen purifier, with special emphasis on operational compatibility with the highly variable demands of an onboard vehicle application.

2. Experimental

2.1. Materials preparation and purifier fabrication

All Pd–Cu films were deposited onto cleaned asymmetric alumina tubes (Kyocera Inc.; 3.2 mm OD × 53 mm length), at a rate of 1–5 Å per second using a DC magnetron sputtering

* Corresponding author. Tel.: +1 908 730 3713; fax: +1 908 730 3198.
E-mail address: dccalabro@exxonmobil.com (D.C. Calabro).

0920-5861/$ – see front matter
doi:10.1016/j.cattod.2006.09.042

unit employing a high purity (>99.9%) Pd–Cu target (60 wt% Pd/40 wt% Cu; Sputtered Films Inc.). Vaporized Pd and Cu atoms deposit onto the alumina substrate creating a thin alloy film having the same composition as the sputtering target (verified to within ±1% by EDS analysis).

To deposit a uniform alloy film around the tube circumference, the alumina tube was attached to a small DC motor inside the vacuum chamber to enable slow rotation during deposition. A 12-V DC bias was applied between the target anode and the metal support to which the alumina tube was affixed. Best results were obtained by the addition of ~10 vol% hydrogen to the argon plasma gas. Final thickness of PdCu alloy deposited by this technique was ~2 microns over a surface area of 5.3 cm^2.

The hydrogenation of trace CO_x in the membrane permeate gas to methane was accomplished using a small tubular reactor packed with crushed and sized (20/40 mesh) commercial steam reforming catalyst. The Haldor Topsoe R-67-7H catalyst containing >12% nickel on a magnesium aluminate spinel was pre-reduced in hydrogen at 400 °C and operated at the same temperature as the membrane.

2.2. Performance testing

The OD sputter-deposited, thin film PdCu membrane, was mounted in a tube-in-shell stainless steel module. High temperature gas tight seals were made using graphite ferrules in compression fittings. Feed gas was introduced into the shell side of the module, purified hydrogen permeate exited via the tube ID. The feed and permeate pressures could be independently varied by proper adjustment of backpressure regulators on both the retentate and permeate gas flow streams. Permeate could be directed either directly to an on-line GC, or to a fixed bed CO_x hydrogenation catalyst bed followed by on-line GC. This arrangement allowed monitoring of the purity of the permeate hydrogen both with and without trace CO_x hydrogenation. The GC detection limits for both CO and CO_2 were established at 10 ppm in hydrogen using a certified gas mixture standard. Typical test conditions with "reformate" feed had a flow of 4 lpm at 10 barg inlet pressure and permeate pressure of 3 barg with membrane and methanation catalyst held at 400 °C. Typical permeate rates of 0.6 lpm were obtained.

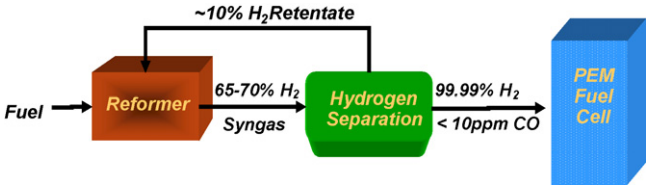

Fig. 1. Process steps for the production, purification and use of hydrogen for power generation [1,3].

3. Results and discussion

The overall process chain for converting a hydrocarbon fuel into electricity is diagrammed in Fig. 1. As described above, the first step is the high temperature steam reforming of the hydrocarbon to a synthesis gas mixture typically containing 65–70% H_2. This mixture is sent to a hydrogen purifier that produces a high purity (>99%) hydrogen stream and a hydrogen-depleted retentate that can be recycled to the reformer (see below). The purifier can consist of a membrane or a pressure swing adsorption unit. This paper will focus exclusively on the use of a dual functional purifier consisting of a dense metal membrane in series with a catalytic methanation reactor for trim CO_x removal [3,4]. Finally, the high purity hydrogen is fed to a PEM fuel cell for reaction with oxygen to generate electricity and water. We will briefly describe the reforming and fuel cell units before discussing the dual functional purifier in more detail.

3.1. Pressure swing reforming: a new way to make syngas

ExxonMobil has recently disclosed a major advance in steam reforming called *pressure-swing reforming* [5–8]. As shown in Fig. 2, this process consists of a fixed catalyst bed operating in a cyclic, alternating flow mode. In the initial operating cycle, a fuel–air mixture is fed to the reactor at low pressure that undergoes combustion thereby generating a hot zone in the bed that migrates in the feed flow direction. At the end of this cycle,

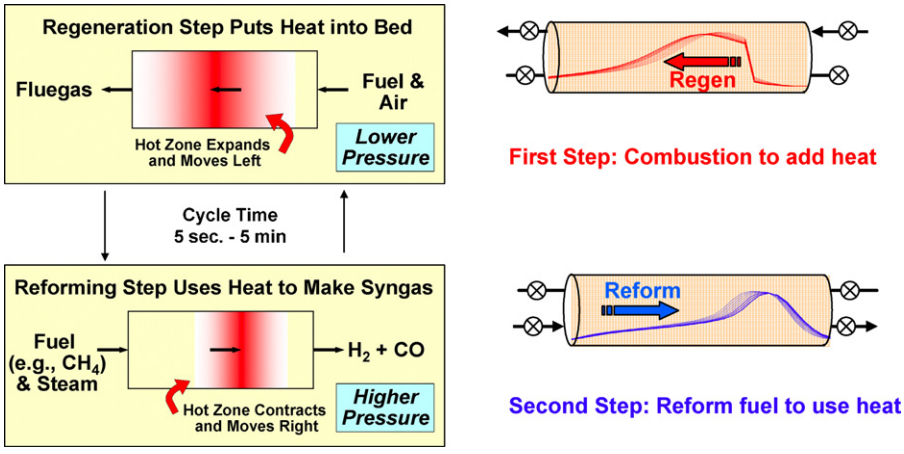

Fig. 2. Pressure swing reforming: a new way to make syngas. A cyclic reactor system moves heat in time from low pressure to high pressure.

the fuel–air feed is stopped and a fuel-steam mixture is fed to the reactor at high pressure from the opposite direction. The hot catalyst bed catalyzes endothermic reforming reactions which consume some of the stored heat generated in the combustion cycle. By alternating between combustion and reforming cycles with careful flow and cycle time control, the hot zone (900–1200 °C) can be confined in the middle of the reactor while maintaining the ends of the reactor at 300–400 °C.

This process scheme has some major advantages compared to conventional autothermal reforming technology. Cyclic combustion and reforming in a single bed provides in situ heat exchange and highly efficient energy capture. With efficient use of the stored heat, no external furnaces are required to pre-heat the air and feed, or for steam generation. These factors result in very low parasitic power loss relative to conventional hydrogen production via sequential autothermal reforming – high temperature water gas shift – low temperature water gas shift – preferential oxidation technology requiring multiple catalyst beds with heat exchange between each process step.

The operation of tandem pressure swing reactors provides a continuous syngas stream. As we will see later when describing an integrated power system, this also provides a continuous combustion bed for recovering the energy value of hydrogen-depleted syngas (membrane retentate), methane by-product from the trim CO_x methanation step in the hydrogen purifier, and O_2 depleted "air" from the cathode exhaust. This capability makes PSR ideally suited for integration with the dual functional purifier described here, and the PEMFC.

3.2. Operational requirements of a vehicular PEMFC

As the engine for a fuel cell vehicle, the operational requirements of the proton exchange membrane fuel cell (PEMFC) establish the performance targets for both the pressure swing reformer and the dual functional purifier. A diagram of a PEMFC is shown in Fig. 3.

A hydrogen fuel cell is an electrochemical device in which H_2 oxidation occurs at the anode generating free protons and electrons. The electrons are available in an external electrical circuit, the protons are transported through an electrically insulating but proton conducting membrane (PEM) to the cathode, where they are reduced in the presence of O_2 to close the electrical circuit and produce water as a by-product. The proton exchange membrane, electrodes, deposited electrocatalysts at the electrode/membrane interfaces, and the gas distribution systems at both electrodes, is collectively referred to as the membrane electrode assembly (MEA). Improvements

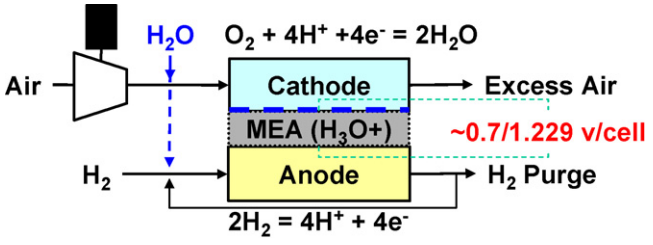

Fig. 3. Basic layout of a proton-exchange membrane fuel cell.

to existing MEA technology is a major hurdle to the advancement of hydrogen power [9–11].

Water management is a critical factor. Proton transfer requires that the membrane exist in a highly hydrated state for two reasons. First, to serve as an effective medium for the rapid transport of hydrated protons (hydronium ions) across the electrode gap, and second, to act as a liquid barrier to neutral gas (either H_2 or O_2) crossover. A major limitation of current PEMFC technology is the maximum operating temperature of the membrane. This limitation is due to both the intrinsic thermal stability of the proton exchange membrane, and its ability to retain a sufficient level of hydration. The most widely used membrane material is a polysulfonated Nafion polymer with a maximum operating temperature of 80–100 °C. At this temperature the platinum anode is highly prone to surface poisoning by CO, which is a major component of syngas. PEM membranes are poisoned at CO levels >10 ppm [12]. This paper assumes a CO target concentration of 10 ppm, however it should be stated that this level has been declining during the course of recent fuel cell development and may continue to do so in the future.

A second operational requirement of the PEMFC is that some manufacturers prefer to feed air to the cathode at elevated pressure under high load conditions. As shown in Fig. 3, a compressor is employed to feed cathode air at pressure, thereby maintaining the oxygen concentration at stoichiometric excess. For systems employing this operation, the efficiency of power generation improves with increasing cathode air pressure up to ~3 bar. Above this pressure, the parasitic power drain of the air compressor exceeds the benefit of further pressure increase. To avoid complications in water management due to variable evaporation rates, substantial pressure gradients within the MEA are not desirable. Therefore, if air is fed to the cathode at 3 bar under high load conditions, the hydrogen feed pressure at the anode must also be capable of approaching 3 bar. We will show below that the need to feed 3 bar hydrogen during high power load conditions in the drive cycle, has major ramifications on the design and operational strategy of the dual functional purifier.

In addition to the above purity and feed pressure requirements of the PEMFC, additional requirements arise in a vehicle application. The DOE target power level for a fuel cell vehicle is 70 kWe at peak power load [11]. This translates into a maximum hydrogen feed rate to the fuel cell of 750 slpm. Referring to Fig. 1, this means that the combined PSR/hydrogen purifier must be scaled to be capable of delivering this hydrogen flux to the PEMFC at peak power load. Furthermore, since the average vehicle drive cycle is highly variable, including multiple start/stop, accelerate/decelerate cycles, overall system durability is critical. Finally, an average 85% recovery of high purity hydrogen at the purifier is required to avoid overall system efficiency loss.

3.3. A dual functional staged hydrogen purifier for an integrated fuel processor–fuel cell power system

The hydrogen purifier described here consists of a dense metal membrane in series with a catalytic methanation reactor.

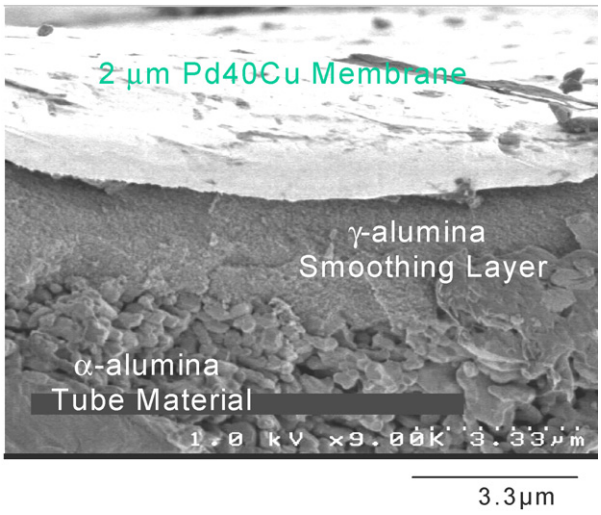

Fig. 4. SEM cross-section of sputter-coated thin film Pd40Cu membrane on porous alumina.

Defect-free Pd alloy foils (10–100 μm thick) are widely used commercially for purifying hydrogen to ultra-high purity levels, however, due to their very high cost, these membranes are not viable candidates for use on a fuel cell vehicle. The membrane employed here consists of a sputter-coated, 2 μm thick, dense Pd40Cu alloy (60 wt% Pd 40 wt% Cu) film supported on an asymmetric porous alumina tubular substrate. A cross-sectional SEM image of this membrane is shown in Fig. 4. The micrograph clearly shows an ~2 μm thick Pd40Cu surface film on a porous alumina substrate. The asymmetric support pore structure is clearly seen as a mesoporous gamma alumina smoothing layer atop a macroporous α-alumina. At this thickness, the supported thin film membrane has increased flux and greatly reduced cost relative to the commercial foil membranes, but is much more prone to defects. The state-of-the-art in thin film Pd alloy membranes is challenged by the fabrication of ever thinner, yet defect-free films.

As stated above, the hydrogen purity requirement of a fuel cell is severe and stringent. Exposure of the anode to CO levels in excess of 100 ppm, will result in significant performance loss due to poisoning of the Pt anode. While this poisoning is slowly reversible, maintaining acceptable drive cycle performance requires that this purity level be sustained over the lifetime of the vehicle. A membrane-only purifier would need to remain defect-free for the duration of its on-board use. This level of durability at a metal thickness that would be economic for a FCV application, has not yet been demonstrated.

Table 1
On line GC analysis of permeate purity with and without downstream CO_x methanation

	Feed (%)	Permeate (%)	After methanation (%)
H_2	65	99.18	97.86
CO	15	0.35	0.001
CH_4			0.83
CO_2	20	0.47	0.001
H_2O			1.30

400 °C, 1 bar, 78,000 GHSV (on methanatorbed).

The dual functional scheme for hydrogen purification illustrated in Fig. 5, has been reported previously [3,4]. The reformate gas product from the pressure swing reformer is fed to the Pd40Cu membrane producing a permeate stream consisting of >99% H_2 and trace levels of CO_x. To generate fuel cell purity hydrogen, this permeate stream is subjected to a second purification step by exposure to a fixed bed $Ni/MgAl_2O_3$ catalyst. This catalyst is shown (Table 1) to be very effective at hydrogenating CO_x to near-extinction according to the reactions shown in Fig. 5 [13,14]. This paper will describe a preferred operational strategy for employing this very effective purification scheme in an on-board hydrogen purifier.

The on-line GC data given in Table 1 shows that passage of the membrane permeate containing >3000 ppm each of CO and CO_2 over the Ni catalyst reduced both of these components to ≤10 ppm. Table 1 also indicates the production of methane and water, consistent with the reactions shown in Fig. 5. For the example given, methanation of the permeate CO_x consumed 2.9% of the hydrogen produced. Keep in mind that the membrane employed here was less than optimal. At reduced CO_x bypass, hydrogen consumption <1% should be achievable. The methane and water by-products lower the final hydrogen concentration, but the critical reduction of CO to the target level is accomplished. As described below, the methane and water by-products are valued in an integrated system.

The above results illustrate the effectiveness of the membrane/methanator purifier. The CO_x level in the permeate is far from being acceptable, indicating substantial defects in the metal membrane. Nonetheless, passage of this permeate through an isothermal methanation catalyst bed at high flowrate (>75,000 GHSV), yields a fuel cell compatible hydrogen stream. The ability to achieve target hydrogen purity with a highly-defected membrane suggests a great benefit in improved on-board system durability. As the membrane selectivity declines with on-board use, the methanator maintains the trace

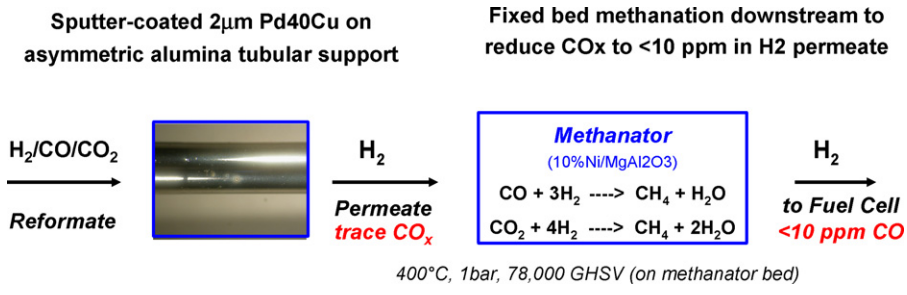

Fig. 5. A two-stage, membrane-methanator hydrogen purifier.

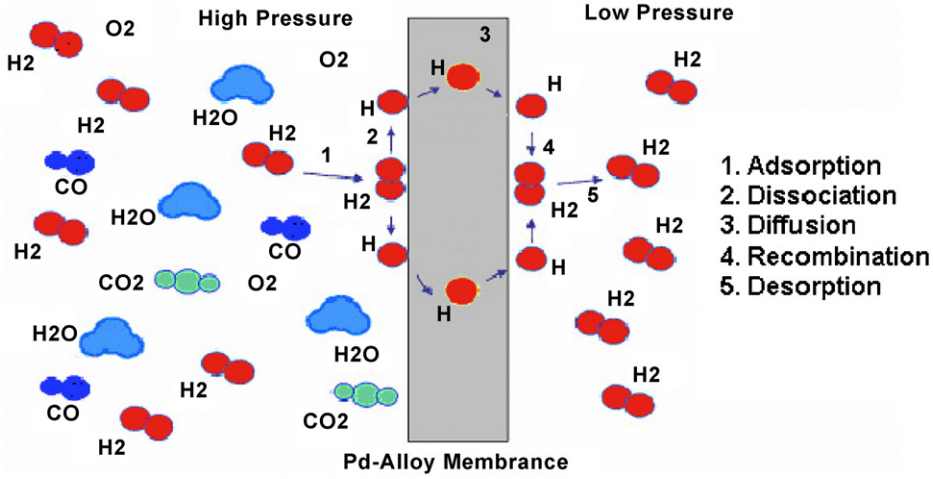

Fig. 6. Solution/diffusion mechanism of hydrogen permeation through a dense Pd alloy membrane.

CO_x at acceptable levels for extended fuel cell performance. The ability to operate both stages in Fig. 5 using adiabatic heat from the PSR, enables heat and space integration for a compact fuel processor/hydrogen purifier. Finally, the methanation by-products are highly valued in the integrated system. Water serves to partially humidify the hydrogen feed to the PEMFC anode, while methane is purged from the anode and recycled to the PSR combustion cycle contributing to energy balance and high overall thermal efficiency.

As described above, the combined fuel processor/purifier system must be able to provide target purity hydrogen at a rate of 750 slpm at peak power load conditions. The basic mechanism of hydrogen permeation through a dense Pd alloy membrane is shown in Fig. 6 [15]. A substantial number of metals and alloys are known to exhibit highly selective hydrogen transport [16]. This property is the basis of dense metal membranes for hydrogen purification. The mechanism of this selective transport is believed due to the ability of molecular hydrogen to dissolve into, then rapidly diffuse through these metals, i.e. solution/diffusion. In Fig. 6, this mechanism is portrayed as a five-step process in which molecular hydrogen initially adsorbs on the metal surface, dissociates to atomic hydrogen which, due to its small size, rapidly diffuses through interstices in the metal lattice to the opposite membrane surface where the atoms recombine prior to final desorption of the reconstituted H_2.

The driving force for the above mechanism is a gradient in hydrogen chemical potential across the membrane. Approximating this driving force as the change in hydrogen partial pressure across the membrane, hydrogen flux is described according to Sievert's law [15] (Eq. (1)),

$$J = F(P^n_{H_2h} - P^n_{H_2l}) = \frac{Q}{l}(P^n_{H_2h} - P^n_{H_2l}) \quad (1)$$

where J = flux, F = permeance, Q = permeability, l = membrane thickness, P_{H_2} = hydrogen partial pressure on high and low pressure sides of the membrane, and n = pressure dependency. The value of n varies between two limiting values, and is broadly indicative of the flux-limiting step of the five-step process described above and in Fig. 6. For relatively thick foils (>5 μm), the flux-limiting step is the rate of diffusion of the hydrogen atoms through the metal lattice. Since the partial pressures in (1) are of H_2, $n = 0.5$ in this case. Alternatively for thin film membranes or when the membrane surface becomes significantly blocked (e.g. poisoning, competitive adsorption), the rate of surface adsorption/desorption and/or dissociation/recombination can become flux-limiting and the value of n approaches 1.

The measured pressure exponent (n) for the membrane used here is shown in Fig. 7. By plotting flux versus driving force and fitting the data to the exponential dependence, we obtain a value of $n = 0.75$ for both a pure hydrogen feed and a mixed $H_2/CO/CO_2$ feed at 400 °C. This n value is reasonable for the 2 μm thick Pd40Cu film used here, and indicates some degree of surface reaction limited flux. Since both the pure and mixed feeds give the same value of n, we cannot attribute $n > 0.5$ to competitive adsorption or surface poisoning. Instead, this value of n may simply reflect the exceedingly fast film diffusion at this thickness, resulting in a flux limited more by the H_2 reactions than the atomic diffusion.

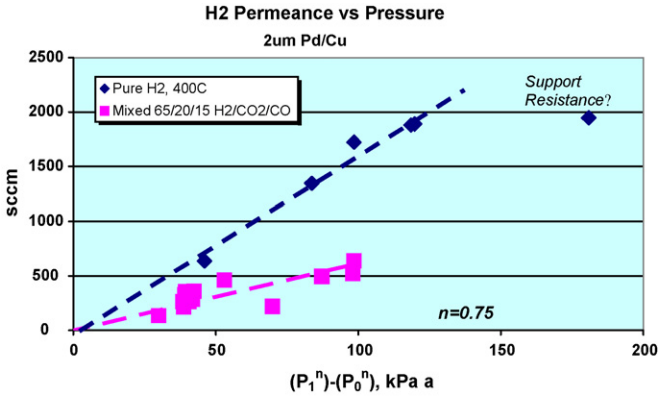

Fig. 7. Flux versus driving force for pure and mixed feeds. Value of n determined by linear least squares fit to hydrogen partial pressures on feed and permeate sides of the membrane.

The data in Fig. 7 also shows a large decrease in flux when comparing the pure to mixed feeds at constant driving force. Since the driving force reflects the change in hydrogen partial pressure, this cannot be attributed to hydrogen dilution in the mixed feed. We attribute this loss of flux on the mixed feed to a boundary layer formation arising from poor flow hydrodynamics in the membrane module [15,17]. We have frequently observed this in lab-scale membrane testing, and caution against attributing mixed feed results to membrane performance until care has been taken to discount the possible presence of boundary layer effects.

Fig. 8 shows experimental flux data obtained on the membrane/methanator purifier described above using mixed, model reformate. The flux units are normalized to the total membrane surface area. The red points are raw data, the blue is corrected for variations in feed rate and ΔP. This data was collected following an extensive lineout on pure hydrogen feed (not shown). The corrected data shows almost 100 h of stable flux of ~400 L/min m^2. Recall that the DOE peak power flux target for a FCV is 750 slpm. The data in Fig. 8 indicates that the membrane used here can achieve this target with ~2 m^2 of surface area.

3.4. Membrane challenge: the drive cycle

The above results indicate that, under laboratory conditions, the two-stage membrane/methanator purifier operating at 400 °C with ~2 m^2 of membrane surface area, can deliver target hydrogen purity and flux. Nonetheless, when subjected to the operating conditions of a vehicle very significant secondary challenges arise. We will see that designing the purifier for greater compatibility with the drive cycle leads us to a major advance in onboard hydrogen purification.

Onboard hydrogen purification using a membrane presents unique challenges relating to the modest permeation driving force available and the highly dynamic nature of the drive cycle. The pressure swing reformer can typically produce outlet pressures of 10–20 bar. Assuming a hydrogen concentration of 65–70%, this delivers a hydrogen partial pressure of 6–12 bar at the membrane inlet. The exiting pressure of the membrane permeate must be equal to or greater than the operating pressure of the fuel cell. Normally the fuel cell operates at, or slightly above, ambient pressure, with some FC system designs employing pressures as high as 3 bar under high load conditions (see above). Subtracting these inlet and outlet pressures leaves an available trans-membrane driving force of 3–11 bar. Note that at constant reformer outlet pressure, the smallest membrane driving force is available under peak power load conditions when hydrogen flux demand is at a maximum.

Under most drive cycle conditions, vehicles operate over a highly dynamic range of power loads, resulting in a highly variable and discontinuous flux demand. To satisfy this operation, the membrane component of the two-stage purifier must be scaled with sufficient surface area to provide peak power flux at minimum ΔP driving force. One result of these design constraints is that for the large majority of the drive cycle, *the membrane surface area is over-sized*. This is illustrated in Fig. 9.

Fig. 9 plots the calculated hydrogen flux as a function of membrane surface area and power load. The data is based on extrapolations of the experimental data shown in Fig. 8 at 400 °C assuming 10 bar reformate pressure and 66.8% H_2. The blue curve represents peak power load conditions with 1500 slpm of reformate feed to the membrane and a permeate pressure of 3 bar. At these conditions, flux increases smoothly with surface area, reaching the target peak power flux of 750 slpm at 2 m^2, as shown in Fig. 8. At this high feed rate, 2 m^2 of membrane recovers only 75% of the hydrogen. Alternatively, the red curve represents a more typical power load. In this case a reformate feed rate of 400 slpm and a permeate pressure of 1.5 bar yields ~230 slpm (25 kWe). Note that this flux is reached using only ~0.3 m^2 of surface area (91% recovery). The remaining 1.7 m^2 of surface must be present to satisfy high load demands, but contributes nothing to hydrogen recovery at average power loads.

The use of a membrane having excess surface area has important consequences as shown in Fig. 10. In this illustration, the membrane is represented as a single tube in shell with feed

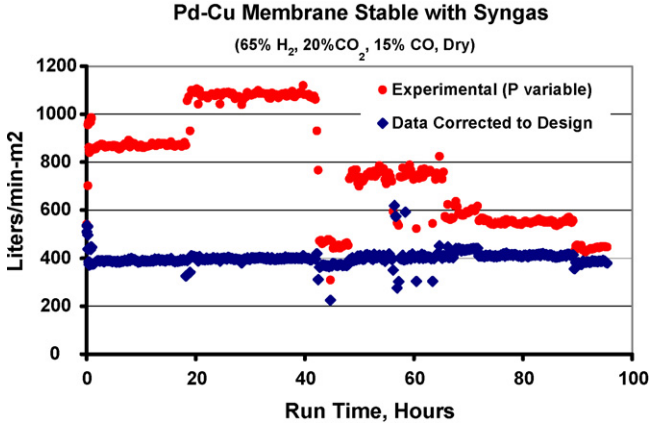

Fig. 8. Membrane surface area normalized flux versus time for the membrane/methanator purifier on mixed feed. Raw data is in red, blue data is corrected for variations in pressure and feed rate.

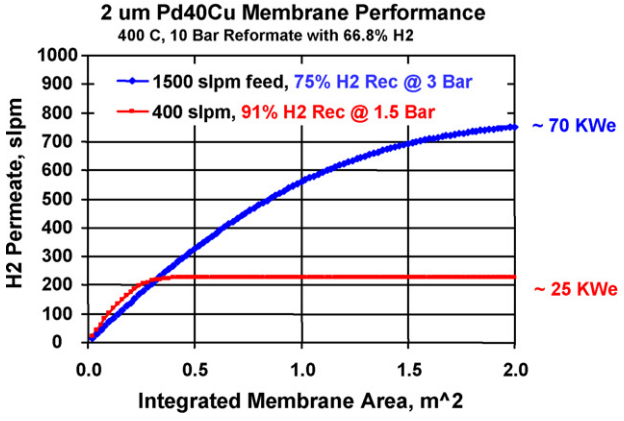

Fig. 9. Hydrogen flux versus membrane surface area at high and average power loads.

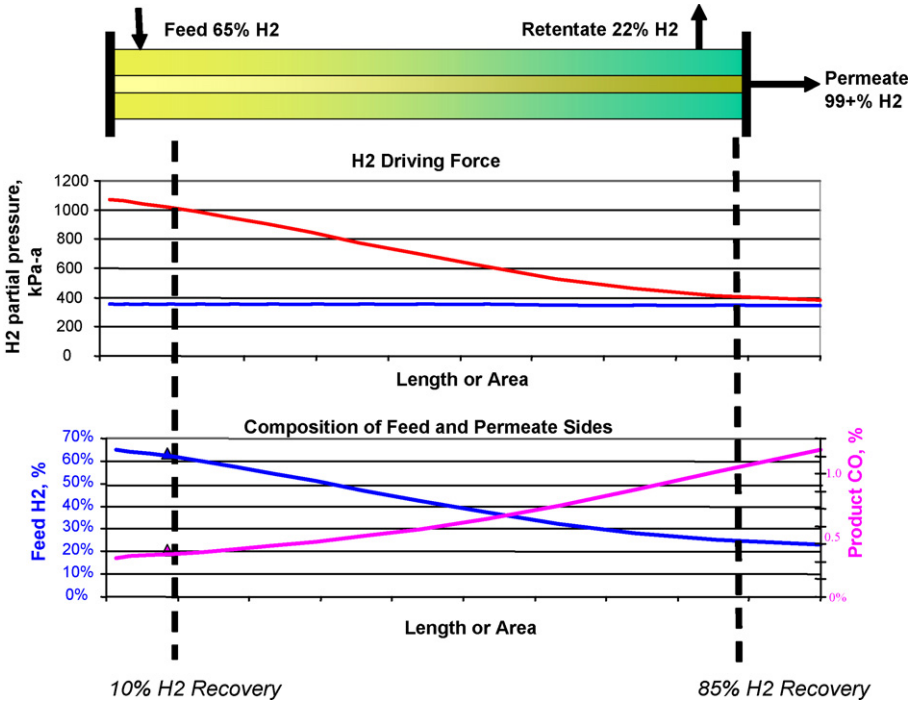

Fig. 10. Surplus surface area and the onset of membrane ‘‘pinch’’. (For interpretation of the references to colour in this figure legend, the reader is referred to the web version of the article.)

entering on the left of the shell side, retentate exiting on the right, and the permeate stream exiting from the tube ID. With hydrogen recovery, the hydrogen partial pressure in the feed side declines as the membrane surface is traversed. This is shown in the top plot of partial pressure versus membrane length where the flat blue curve represents the constant partial pressure on the permeate side, and the decreasing red curve (feed partial pressure) decays as hydrogen transports across the membrane. The difference between these curves is the permeation driving force, if this decays to zero before the feed stream reaches the retentate outlet, the membrane is said to be ‘‘pinched’’.

The use of an over-sized membrane having surface area that is not contributing to the hydrogen recovery is not only inefficient, but may also be damaging to the product purity. The bottom plot in Fig. 10 shows the change in relative concentrations of hydrogen (blue; decreasing) and CO (red; increasing) along the membrane length. As we saw above, as hydrogen permeates the membrane, it’s concentration on the feed side decreases. An obvious outcome of this is that the relative concentration of everything else in the feed increases. This creates an increasing driving force for the non-selective transport of impurities. As the degree of membrane pinch increases, the extent of purity loss via defect flux increases. As shown in Fig. 9, these conditions are present during the large majority of the drive cycle (25 kWe).

As we have seen, scaling the membrane to accommodate the extremes of hydrogen flux creates a condition of surplus surface area and the potential for purity loss due to membrane pinch. This situation is unavoidable due to the dynamic range of the drive cycle. We now turn to an approach that makes beneficial use of this surplus membrane area.

3.5. Staged recovery and onboard hydrogen storage

Two major challenges for fuel cell vehicle technology featuring on-demand hydrogen production are system start-up time and responsiveness to sudden load spikes. Starting a hydrogen fuel cell requires an instantaneous source of high purity hydrogen. Since all reformers have a non-zero start-up time, an alternate, readily available source of hydrogen is needed, suggesting the use of a small, pressurized hydrogen storage buffer. In addition to system start-up, a source of high pressure hydrogen could be used to supplement the on-board processor/purifier under transient, high load conditions when the fuel cell is operated at elevated pressure.

A membrane-based purifier is challenged to deliver high pressure hydrogen since it relies on a pressure-drop driving force favoring the production of a low pressure permeate. The delivery of a high pressure permeate in the absence of a commensurate increase in feed pressure, can only be accomplished at lower flux, and, if additional surface area is not available, reduced hydrogen recovery. We have shown that the dynamic drive cycle forces the use of an over-sized membrane for on-board hydrogen purification. It is this surplus membrane surface area that can be used to deliver high pressure hydrogen.

We introduce here the use of a multi-stage hydrogen membrane/methanator recovery. It is shown that this imparts great flexibility in the operation of the purifier/fuel cell system, and avoids the surface area mismatch conditions described above. The use of a multi-stage membrane system enables operation of some fraction of the total membrane surface area for hydrogen recovery at pressures substantially approaching that of the feed hydrogen partial pressure. This source of on-

board high pressure hydrogen can then be optionally fed to an on-board storage device for use during vehicle startup, or to the fuel cell, either directly or via the storage device, under high power load conditions.

Fig. 11 illustrates a two-stage recovery of purified hydrogen that employs two membrane/methanator units in series (the methanator is omitted for clarity), one feeding a static storage buffer to be used on-demand, the other feeding permeate directly to the PEMFC. [*Note*: In the following discussion of staged recovery, the presence of the methanation catalyst on the permeate side of the membranes is to be understood.] Feed synthesis gas from the PSR having a hydrogen partial pressure of ~6.5 bar enters the first membrane. The permeate of this membrane delivers high purity hydrogen to a 10 L storage buffer. The buffer exits via a bleed valve to the hydrogen inlet of the fuel cell. The hydrogen-depleted retentate from this first membrane cascades to the inlet of the second membrane, the permeate of which is fed directly to the inlet of the fuel cell. The fuel cell inlet pressure range of 1.5–3 bar, establishes the permeate pressure of the second stage membrane. The difference between this pressure and the hydrogen partial pressure of the hydrogen-depleted stream from the first stage membrane, is the driving force across the second stage membrane.

Initially, when the storage buffer is empty, a maximum difference in hydrogen pressure, and therefore a maximum hydrogen flux, exists across the first stage membrane. With the buffer bleed valve closed, the buffer pressure increases as recovered hydrogen is fed to it from the first membrane, thereby decreasing the pressure delta and hydrogen flux across the membrane. Finally, as the pressure of the buffer approaches the hydrogen partial pressure of the feed to the first stage membrane, the driving force for flux decays to zero. This is not membrane pinch since we have not lost the driving force as a result of depleting the feed side hydrogen concentration, and the relative driving force for impurity flux has not increased. In this static mode of operation, the buffer is fully pressurized and the feed passes through the first stage membrane unchanged.

Simulations of hydrogen recovery for this static buffer mode are also shown in Fig. 11. These plots were generated at the same average load conditions (25 kWe) used in Fig. 9 using the same total membrane surface area (2 m^2) divided into two 1 m^2 stages. The graph on the left shows the percent hydrogen recovery from both stages during buffer filling. The shapes of these curves change continuously as the buffer pressure increases, the plot shown is for an instantaneous buffer pressure of 5 bar. The simulation shows that under these conditions, both membranes are pinched at hydrogen recoveries of 50% and 41% in the two stages. Given the flux across the first membrane (blue curve; 0–1 m^2), pressurizing the buffer should take substantially less than 30 s, after which the graph on the lower right pertains. In this case, the buffer is fully pressurized resulting in zero flux driving force across the first stage membrane. In effect, the first 1 m^2 of membrane surface area has been taken out of operation, nonetheless the second stage membrane alone is still more than sufficient to recover 91% of the synthesis gas hydrogen that has cascaded through both membranes.

The two stage recovery shown in Fig. 11 provides two major advantages relative to a single stage hydrogen recovery. First, by utilizing a portion of the membrane surface area to recover hydrogen at elevated pressure, the capability of storing high pressure hydrogen on-board the vehicle is realized. Second, the ability to effectively remove a significant fraction of the total membrane surface area from operation for most of the drive cycle by dead-ending its outlet to the static buffer, greatly reduces the extent of membrane pinch and the potential for purity loss. We have illustrated these benefits using a 50/50 membrane area staging. Note that the rate of buffer pressurization and the reduction in pinched surface area can both be improved further by a >50/<50 staging. The preferred staging ratio would derive from a total, integrated system optimization.

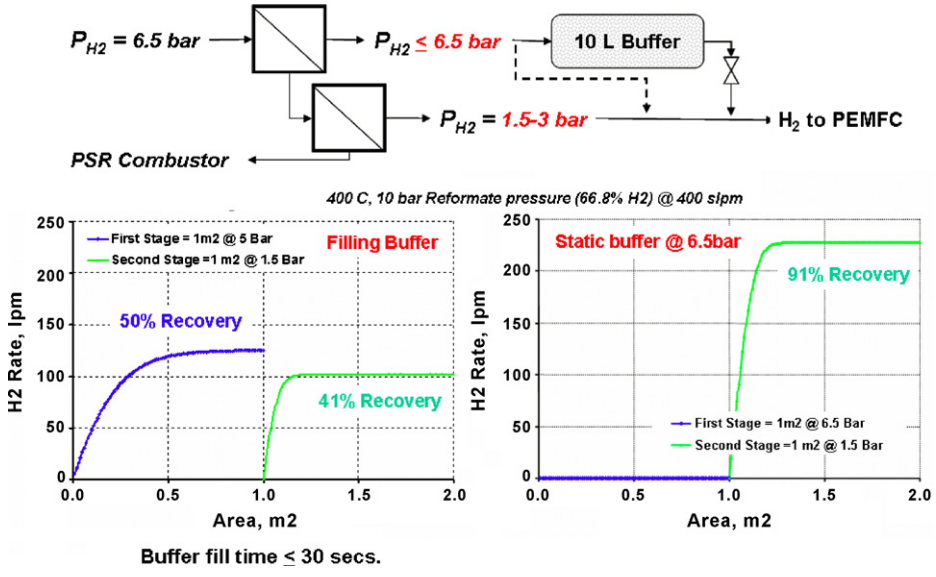

Fig. 11. Staged hydrogen recovery with static buffering.

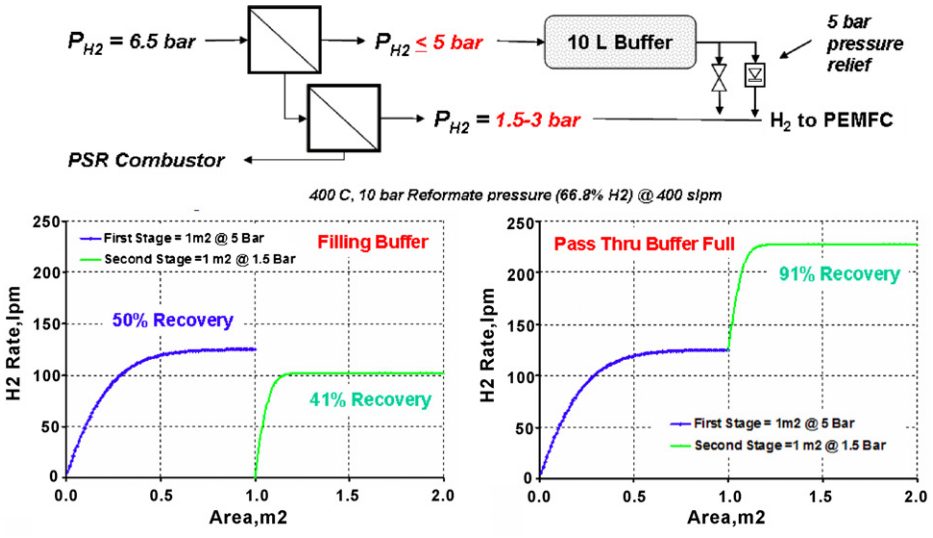

Fig. 12. Staged hydrogen recovery with dynamic buffering.

Fig. 12 shows an alternative operational mode to that shown in Fig. 11 in which, rather than sequestering the buffer hydrogen, it is used dynamically throughout the drive cycle. This is done very simply by supplementing the bleed/shutoff valve at the buffer exit with a pressure relief valve. Assuming the relief valve is set to a pressure that is lower than the feed hydrogen partial pressure to the first membrane, a non-zero driving force will be maintained across this membrane. The buffer pressure will rise to the setpoint relief pressure, at which point hydrogen will discharge from the buffer to the fuel cell inlet to maintain the setpoint pressure in the storage buffer.

In this case, the recovery curves during buffer filling (Fig. 12, bottom left) are identical to those in Fig. 11 for the static mode. By contrast, since both membranes maintain a non-zero flux even after the buffer has reached the setpoint pressure, the hydrogen flux remains additive for the multiple stages (Fig. 12, bottom right).

The two configurations disclosed for the staged recovery concept provide different pros and cons that make them appropriate for different overall system designs. The ‘‘static’’ scenario has the benefits of charging the buffer to the maximum possible pressure, and a greater reduction in overall membrane pinch. The downside of this operation is that the methanator bed directly downstream of the first membrane, is only maintained at reaction temperature by the flow of hot permeate. Once the static buffer is fully pressurized the flux across membrane one goes to zero and its downstream methanator no longer has a source of heat. Unless a means of providing auxillary heat is available, the first stage methanator temperature will drop below reaction temperature during extended drive times when buffer hydrogen is not used. Alternatively, the ‘‘dynamic’’ buffer scenario avoids the methanator cooling problem by maintaining a continuous, non-zero flux across both membrane stages, but does not achieve as high a buffer pressure or as great a membrane pinch reduction as the static buffer.

3.6. An integrated fuel processor–fuel cell power system

As shown in Fig. 1, a hydrogen-powered fuel cell requires the production and purification of hydrogen. This is true regardless of scale or application. In the case of distributed power systems such as vehicular or remote applications, substantial benefits arise from combining the fuel processing/hydrogen purification/fuel cell components into an integrated system fueled by the existing hydrocarbon infrastructure. At ExxonMobil we have demonstrated pressure swing

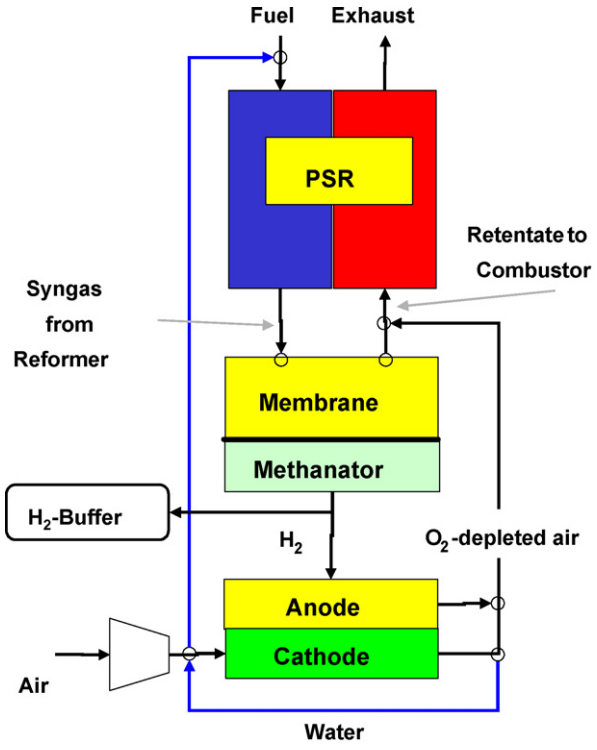

Fig. 13. An integrated pressure swing reformer/membrane–methanator–buffer/PEMFC power system.

Table 2
Calculated energy balanced thermal efficiencies for the integrated PSR–membrane/methanator–PEMFC system

	Heat balanced 25 °C feed/product	Heat balanced 80 °C process H_2O 300 °C exhaust	Energy balanced system
Reformer thermal efficiency (%)	89	80	70
Fuel cell thermal efficiency (%)	60	60	60
Efficiency, net % kWe/kW HC LHV	54	48	42

System simulations: 60% FC efficiency (assumes H_2 LHV).

reforming, and promoted staged hydrogen recovery, as technologies ideally suited to this integrated power system.

Fig. 13 shows an integrated PSR/membrane–methanator–buffer/PEMFC system. This system runs on conventional hydrocarbon fuels and air to produce a combustion exhaust and electricity. All purge streams from the membrane/methanator and the fuel cell are utilized by the pressure swing reformer to produce high pressure syngas. A two-stage purifier, each stage consisting of a Pd40Cu alloy membrane and a Ni CO_x methanation catalyst, produces target hydrogen purity and flux, and enables the recovery and storage of high pressure hydrogen.

Table 2 shows the overall calculated system efficiency for the above system. All of these calculations assume 60% thermal efficiency for the fuel cell [11]. The reformer thermal efficiency was calculated using three sets of assumptions. The left column of numbers assumes a fully heat balanced PSR (heat generated in combustion exactly equals that consumed in reforming) with the feed and product streams entering and exiting at 25 °C. We have calculated and experimentally verified a thermal efficiency of 89% for the PSR using these assumptions [7]. If the same calculation is done assuming 80 °C process water and a 300 °C exhaust, the calculated efficiency drops to 80%. Finally, the right hand column assumes a 10% efficiency loss due to heat and parasitic power losses (air compressor, FC cooling), dropping the energy balanced reformer efficiency to 70%. Multiplication by the assumed 60% fuel cell efficiency gives a total integrated system efficiency of 42%.

4. Conclusions

An integrated fuel processor/fuel cell distributed power system is proposed having a projected overall thermal efficiency in excess of 40%. This system consists of a pressure swing reformer running on commercial hydrocarbon fuels to produce a reformate gas mixture, a dual functional membrane/methanator separator to produce high purity hydrogen, and a proton exchange membrane fuel cell.

Pressure swing reforming (PSR) is shown to be a major advance in small-scale hydrogen production. As an *in situ* heat exchange process, PSR avoids the thermal losses associated with feed pre-heating and downstream heat exchange, resulting in superior thermal efficiency relative to conventional ATR technology.

A dual functional hydrogen purifier is shown to provide peak power hydrogen flux and fuel cell purity in a compact, on-board unit. Specifically, 2 m^2 surface area of a supported 2 μm thick Pd40Cu alloy membrane can deliver 750 slpm of hydrogen at low ΔP (∼3.5 bar) driving force. Subsequent passage of this permeate stream through a packed Ni/$MgAl_2O_3$ catalyst bed at >75,000 GHSV converts trace CO_x levels to ≤10 ppm each of CO and CO_2.

Membrane surface area must be sized for peak power flux at minimum ΔP driving force, resulting in over-sized membrane surface for most of the drive cycle. This surplus surface area can be employed in a staged hydrogen recovery scheme that increases the compatibility of the membrane operation with the dynamic drive cycle. More significantly, staged recovery enables operation of some fraction of the membrane surface area at pressures substantially approaching that of the feed hydrogen partial pressure. This creates an onboard source of high pressure hydrogen to be optionally fed to a storage device for use during vehicle startup, or to the fuel cell, either directly or via the storage device, under high power load conditions.

The ability to generate and purify a source of high pressure hydrogen remotely, is a major advance in the use of distributed fuel processing for fuel cell vehicle technology development.

Acknowledgements

The authors greatly appreciate the technical contributions of Bruce Ballinger, Stanley Jakubowicz and Paul Tindall in the fabrication and evaluation of the membrane and dual functional module.

References

[1] D.J. Edlund, W.A. Pledger (Idatech, LLC) US patent 6,994,927 (2006).
[2] I. Masatoshi, I. Yasukazu, (Nissan Motor Co.) US patent 6,841,280 (2005).
[3] D.J. Edlund, US patent 5,861,137 (1999).
[4] M.L. Doyle, N. Edwards, (Johnson Matthey) US patent 6,350,297 (2002).
[5] F. Hershkowitz, H.W. Deckman, (ExxonMobil Corp.) US patent application 2003/0235529 A1 (2003).
[6] F. Hershkowitz, P.J. Berlowitz, R.D. Partridge, (ExxonMobil Corp.) US patent application 2004/0175326 A1 (2004).
[7] F. Hershkowitz, P.J. Berlowitz, H.W. Deckman, E. Marucchi-Soos, C.S. Gurciullo, J.W. Frederick, N. Rados, R. Agnihotri, Proc. Fuel Cell Topical Conference, AICHE Annual Meeting, November 2004, paper 23D.
[8] F. Hershkowitz, P.J. Berlowitz, R.F. Socha, E. Marucchi-Soos, J.W. Frederick, Proc. AICHE Annual Meeting, New York, NY, 2005.
[9] R.F. Service, Science 312 (2006) 35.
[10] A.H. Tullo, Chem. Eng. News (2005) 18.
[11] E.J. Carlson, P. Kopf, J. Sinha, S. Sriramulu, Y. Yang, National Renewable Energy Laboratory, subcontract report NREL/SR-560-39104, December 2005.

[12] U.S. Department of Energy Office of Hydrogen, Fuel Cells & Infrastructure Technologies, DOE Workshop on Hydrogen Separation and Purification Technologies, Arlington, VA, September 8–9, 2004.
[13] C.H. Bartholomew, in: Z. Paal, P.G. Menon (Eds.), Hydrogen Effects in Catalysis, Fundamentals and Practical Applications, Marcel Dekker, New York, 1988 , p. 543 (Chapter 20).
[14] C.-W. Hu, J. Yao, H.-Q. Yang, Y. Chen, A.-M. Tian, J. Catal. 166 (1997) 1.
[15] J.P. Collins, J.D. Way, I&EC Res. 32 (1993) 3006.
[16] F.A. Lewis, The Palladium Hydrogen System, Academic Press, 1967 .
[17] A. Mourgues, J. Sanchez, J. Membr. Sci. 252 (2005) 133.